

9. Dhar, A. K., Roux, M. M. and Klimpel, K. R., Detection and quantification of infectious hypodermal and hematopoietic necrosis virus and white spot virus in shrimp using real-time quantitative PCR and SYBR green chemistry. *J. Clin. Microbiol.*, 2001, **39**, 2835–2845.
10. Nataraja, K. N. and Jacob, J., Clonal differences in photosynthesis in *Havea brasiliensis*, Mull. Arg., *Photosynthetica*, 1999, **36**, 89–98.
11. Ratcliff, F., Martin-Hernandez, A. M. and Baulcombe, D. C., Tobacco rattle virus as a vector for analysis of gene function by silencing. *Plant J.*, 2001, **25**, 237–245.
12. Lu, R., Martin-Hernandez, A. M., Peart, J. R., Malcuit, I. and Baulcombe, D. C., Virus-induced gene silencing in plants. *Methods*, 2003, **30**, 296–303.
13. Lacomme, C., Hrubikova, K. and Hein, I., Enhancement of virus-induced gene silencing through viral-based production of inverted-repeats. *Plant J.*, 2003, **34**, 543–553.
14. Tao, X. and Zhou, X., A modified viral satellite DNA that suppresses gene expression in plants. *Plant J.*, 2004, **38**, 850–860.

ACKNOWLEDGEMENTS. We thank S. P. Dinesh-Kumar, Yale University, USA for VIGS vectors. The research was supported by the Council of Scientific and Industrial Research (CSIR), New Delhi.

Received 14 February 2005; revised accepted 14 October 2005

Cation distribution in Cr-spinels from the Sittampundi layered complex and their intracrystalline thermodynamics

Sachinath Mitra¹, Maibam Bidyananda^{2,*} and Asok Kumar Samanta¹

¹Department of Geological Sciences, Jadavpur University, Kolkata 700 032, India

²Department of Geological Sciences, Gauhati University, Guwahati 781 014, India

High aluminium chromites occur as bands within anorthosite layered complex of Sittampundi (Tamil Nadu). Cation distribution of two chromite samples is determined by combined electron probe microanalysis and Mössbauer spectroscopy. In the deconvolution of the Mössbauer spectra, the suitability of the best model of spectral fitting has been established with the observation that both Fe²⁺ and Fe³⁺ ions occur at tetrahedral (A) and octahedral (B) sites and Fe³⁺/ΣFe found to be ranging between 0.45 and 0.48. Oxygen fugacity (*f*O₂) has been determined to be about 10^{-7.3}. Thermodynamic parameters have been determined for the studied chromites using standard models.

Keywords: Cation distribution, chromite, Mössbauer spectroscopy, Sittampundi, thermodynamic parameter.

SPINELS are used as a petrogenetic indicator because their chemical and structural variations are dependent on the

paragenesis, pressure and temperature of crystallization. The widespread occurrence of spinels is in part a result of the large number of cations that the structure can accommodate. Many crystallographic^{1–4} and thermodynamic^{4–10} studies have been done on synthetic spinels because of their applications in materials science, metallurgy and earth sciences. However, studies on natural spinel are scarce due to difficulties in assigning major cations present in the tetrahedral (A) and octahedral (B) sites. Among the cations present in spinel, Fe commonly exists in multiple valence states and accurate knowledge of the Fe³⁺/Fe²⁺ ratio allows us to estimate the oxygen fugacity (*f*O₂), which controls the magmatic crystallization path and composition of the resulting mineral phases. The aim of the present work is to determine the cation distribution of chromites (Cr-spinel) from the Sittampundi complex, Tamil Nadu, using electron probe microanalysis (EPMA) and room temperature ⁵⁷Fe Mössbauer spectroscopy (MS) and the intracrystalline thermodynamic parameters of the natural samples.

Sittampundi layered anorthosite complex occurs as a layered igneous body¹¹. The study area forms a part of the granulite terrain of South India. Major rock types are chromitite bearing meta-anorthosite, amphibolite, basic granulite, two pyroxene granulite, leptynite, biotite gneiss and pink granite. Chromitite occurs exclusively within the anorthosite as discontinuous bands/lenses. Samples used for crystallo-chemical investigation were culled from chromitites (chromite + rutile + calcic amphibole ± antho-phyllite ± clinocllore). Two samples, #30a and #56 were collected from conformable chromitite lenses on a foot track in the western part of Karungalpatti, Salem district, Tamil Nadu. These two samples are henceforth referred to as Ch₁ and Ch₂.

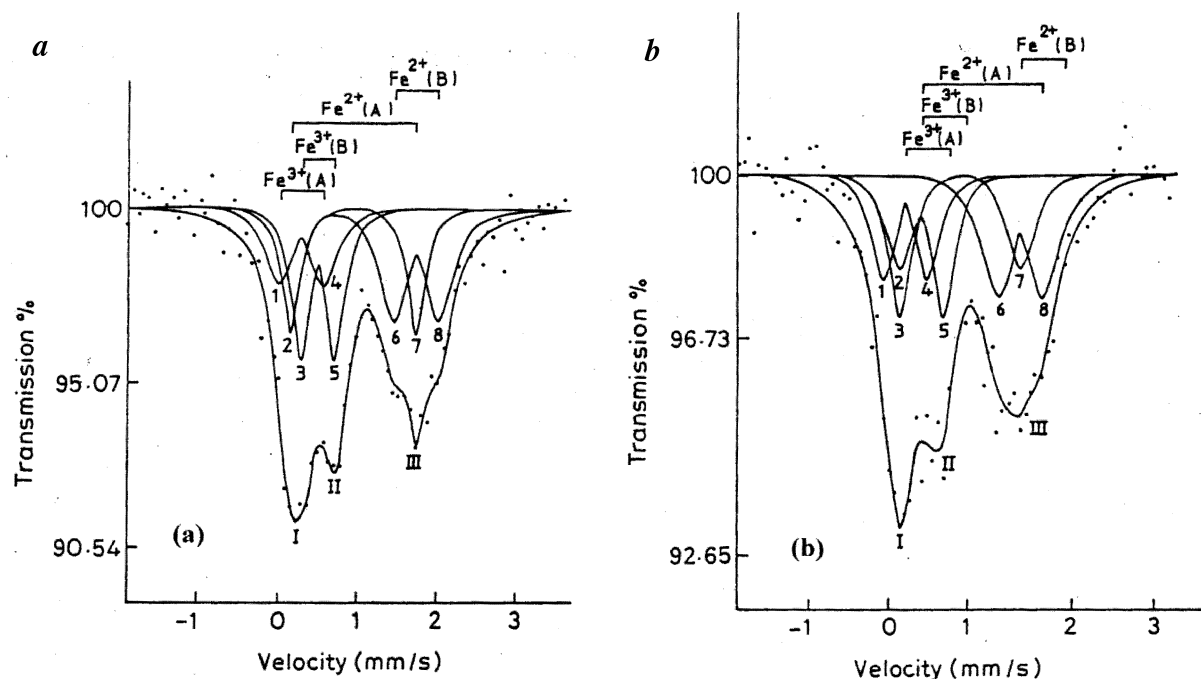
Chromite samples from the Sittampundi area were studied by the combined EPMA and MS. Samples were analysed by a JEOL-733 superprobe microanalyser with wavelength dispersive method at the Department of Geology, Yonsei University, Seoul. Room temperature (298 K) Mössbauer spectrum was recorded in a Wissel-make conventional constant acceleration spectrometer using a 10 mCi Co/Rh source. The spectrum was fitted to Lorentzian lines with a nonlinear least square fit programme. The velocity calibration was performed with respect to pure metallic iron (99.99%) standard. Detailed processing of the samples and the procedures adopted for data acquisition for the EPMA and MS studies are reported elsewhere¹².

Natural chromite samples having complex compositions or crystallizing in an oxidizing environment, often exhibit disorder of Fe²⁺ and Fe³⁺ distribution between octahedral (B) and tetrahedral (A) sites. We have fitted the spectra considering both the normal and disordered distribution. The spectra fitted in the disordered distribution showed better acceptable *c*². For natural chromites best-fitting results were obtained using a three-doublet model by Wood and Virgo¹³ and a four-doublet model by Dyar *et al.*¹⁴. Fitting model with four doublets showed better results and

*For correspondence. (e-mail: bmaibam@yahoo.com)

Table 1. Mössbauer parameters and distribution of Fe²⁺ and Fe³⁺ at different sites and Fe³⁺/ΣFe determined from relative areas

Sample no.	IS (mm/s)	QS (mm/s)	Site	Line width (Γ) (mm/s)	Area (%)	χ ²	Fe ³⁺ /ΣFe
Ch ₁	0.31	0.53	Fe ³⁺ (A)	0.46	20.56	1.61	0.48
	0.53	0.43	Fe ³⁺ (B)	0.33	27.66		
	0.95	1.62	Fe ²⁺ (A)	0.30	20.63		
	1.74	0.58	Fe ²⁺ (B)	0.49	31.15		
Ch ₂	0.22	0.55	Fe ³⁺ (A)	0.40	20.45	2.48	0.45
	0.44	0.52	Fe ³⁺ (B)	0.36	24.49		
	0.90	0.52	Fe ²⁺ (A)	0.46	21.25		
	1.66	0.56	Fe ²⁺ (B)	0.57	33.81		

**Figure 1.** Room temperature ⁵⁷Fe Mössbauer spectra of chromites: (a) sample Ch₁ and (b) sample Ch₂.

is considered for the present study. The obtained hyperfine parameters and Fe³⁺/ΣFe ratios are presented in Table 1 and the spectra are shown in Figure 1.

The first doublet (1–4) with IS 0.31 mm/s (sample Ch₁) and 0.22 mm/s (sample Ch₂) has been assigned to tetrahedral Fe³⁺. These values correspond to the results reported by earlier workers^{14–20}. Doublets (3–5) with IS 0.53 mm/s (sample Ch₁) and 0.44 mm/s (sample Ch₂) are assigned to octahedral Fe³⁺, which is in accordance with reported by previous workers^{16,17,20}.

Galvao Da Silva *et al.*¹⁶ have assigned the doublets with IS 0.80–1.00 mm/s and QS 1.36–1.70 mm/s to Fe²⁺ ↔ Fe³⁺ + e⁻ at B site (electron-hopping). Similar electron-hopping in chromite was also reported by Fatseas *et al.*¹⁵, with a lower isomer shift value. However, subsequent workers have discarded the concept of electron-hopping in

spinel^{14,17,18,21,22} and assigned the doublets with IS 0.85–0.95 mm/s to tetrahedral^{14,17,21} Fe²⁺ and QS^{14,21} ranging from 0.75 mm/s. In the present case the doublets (2–7) with IS 0.95 mm/s (sample Ch₁), 0.90 mm/s (sample Ch₂) and the corresponding QS of 1.62 and 0.52 mm/s respectively, are assigned to Fe²⁺ at A-site rather than Fe²⁺ ↔ Fe³⁺ at B-site^{14,17–19,21}, favouring the view that the present samples showing such hyperfine parameters do not involve Fe²⁺ ↔ Fe³⁺ electron hopping.

Assignment of the fourth doublet (6–8) with IS 1.74 mm/s (sample Ch₁) and 1.66 mm/s (sample Ch₂) may be debatable. Early workers^{15,16,23,24} had assigned doublet with IS 1.08 mm/s to Fe²⁺ (A). Subsequent studies on spinels, however, assigned the doublet with IS ≥ 1.02 mm/s to Fe²⁺ at B-site^{14,17–20}. The presence of four sets of doublets and estimated Fe³⁺/ΣFe ratios (Table 1), show the oxi-

dized nature of the Sittampundi chromites. Chemical composition of the studied chromites and cation distribution based on combined EPMA and MS studies are presented in Table 2.

Spinel occurs in two types: (i) normal, where divalent cations occupy tetrahedral site and trivalent cations occupy octahedral site and (ii) inverse, where trivalent cations occur in tetrahedral site and octahedral site is occupied by both divalent and trivalent cations. Any partly disordered state may be expressed as a mix of these two end-members, with a general formula $^{[4]}(A_{1-x}B_x)^{[6]}(B_{2-x}A_x)O_4$, where x is the degree of disorder. Characterization of order-disorder phenomenon is central to the understanding of the thermodynamic properties of spinels. So far, application of the postulated thermodynamic models to natural samples is limited. From the combined EPMA and MS data, we have estimated the thermodynamic parameters of the studied samples. Absence of olivine-spinel assemblage does not allow us to determine the equilibrium temperature of the studied chromite samples. We have estimated these equilibrium temperature of an associated basic granulite rock. Using garnet-clinopyroxene geothermometry²⁵, equilibrium

temperatures of 950°C (core) and 740°C (rim) are obtained for a heterogenous garnet. We have used the two temperatures for thermodynamic calculations. It can be noted that the calculated intracrystalline thermodynamic parameters of the Sittampundi chromites may not be immediately comparable with the reported synthetic spinel data because of the complex chemistry of the studied samples (Table 2).

In spinel, the degree of exchange between tetrahedral and octahedral sites can be quantified by the degree of disorder, x , giving the fraction of trivalent cations in the tetrahedral site. Complete order has x value of 0 and a value of 1 represents a completely disordered state. For the studied samples, x is found to be 0.38 (Ch₁) and 0.53 (Ch₂), showing their disordered nature. The oxygen positional parameter (u) is sensitive to changes in cation distribution and follows a similar path on heating as the degree of disorder²⁶. Oxygen parameter of the studied samples has been estimated using the 3rd polynomial equation, $u = 0.26488 - 0.00118x - 0.0289x^2$. The two determined u values of 0.256137 (Ch₂) and 0.260258 (Ch₁) are close to the reported values of the 2–3 spinels^{8,27}; however they are less than that of the measured Nuggihalli chromite (0.2623)²⁸.

Navrotsky and Kleppa²⁹ sought a co-relationship between the interchange enthalpy (ΔH_{int}) and the equilibrium cation distribution as a function of temperature. According to them, a knowledge of the equilibrium cation distribution at a temperature is sufficient to estimate interchange enthalpy. For calculation of the parameter, we have used the equation $\Delta H_{int} = -RT \ln[x^2/(1-x)(2-x)]$, where R is the gas constant and the enthalpy of disordering (ΔH_{dis}) is assumed to be the product of degree of disordering and interchange enthalpy. The two enthalpies are calculated for the Sittampundi chromites (Table 3).

The driving force in forming a solid solution is usually configurational entropy of mixing. A solid solution like natural chromite (Cr-spinel) will only be stable if its free energy is less than that of an equivalent mechanical mixture of its components, or of any possible exsolution product. Spinel with a random or highly inverse cation distribution generally have more positive entropy than the largely normal spinels²⁹. Calculated configurational entropy due to positional disorder of the cations for the samples using Navrotsky and Kleppa model²⁹ is presented in Table 3. Positive entropies of the Sittampundi chromites result due to configurational disorder resulting from the mixing of different cations on equivalent structural sites. The values are plotted against the degree of disorder³⁰ and show their distinct disordered nature (Figure 2).

At equilibrium, interchange enthalpy equals to $a + 2bx$, where a and b are the disordering energy and the value of b for 2–3 spinels is taken as -20 kJ/mol⁹. Using the two metamorphic equilibrium temperatures (950 and 740°C), a is calculated for the studied samples. The values of a at the two temperatures for sample Ch₂ are 30.347 and 28.799 kJ/mol, and for sample Ch₁ are 34.981 and 32.565 kJ/mol, respectively (Table 3).

Table 2. Cation distribution of studied chromites using electron probe microanalysis and Mössbauer spectroscopy (MS)

Oxide	Ch ₁ *	Ch ₂ *
SiO ₂	0.01	0.15
TiO ₂	0.16	0.12
Cr ₂ O ₃	34.68	36.72
Al ₂ O ₃	28.06	25.56
Fe ₂ O ₃	14.26	14.34
FeO	13.77	15.80
MnO	0.23	–
MgO	10.03	7.60
NiO	0.14	0.17
CaO	–	0.17
Na ₂ O	0.02	0.02
K ₂ O	0.01	0.01
Total	101.37	100.66
Number of cations on the basis of 32 oxygen		
A-site		
Fe ²⁺	1.145	1.307
Fe ³⁺	1.141	1.258
Al	1.901	2.473
Mg	3.726	2.891
Mn	0.045	–
Ni	0.030	0.035
Na	0.010	0.009
K	0.002	0.002
Ca	–	0.025
B-site		
Cr	6.823	7.442
Al	6.329	5.245
Fe ²⁺	1.729	2.079
Fe ³⁺	1.536	1.506
Ti	0.032	0.031
Si	0.003	0.046

Distribution of Fe into FeO and Fe₂O₃ is based on room temperature MS. *Average of seven spots.

Table 3. Thermodynamic parameters of Sittampundi chromites

<i>T</i> (K)	ΔH_{int} kJ/mol	ΔH_{dis} kJ/mol	ΔG_{dis} kJ/mol	a_1 kJ/mol	a_2 kJ/mol	a kJ/mol
Sample Ch ₁ : $x = 0.38$; $u = 0.260258$, $S_{conf} = 13.679$ J/mol K						
when $r_1 = [Fe^{3+}]$, $r_2 = [Al]$						
1225	19.741	7.521	24.279	14.044	23.306	34.981
1013	16.325	6.220	20.077	14.251	21.910	31.565
when $r_1 = 1 - ({}^{[4]}X_{Mg} + 2{}^{[4]}X_{Mg})$, $r_2 = 1/2({}^{[4]}X_{Al} + 2{}^{[6]}X_{Al})$						
1225	19.741	7.521	24.279	56.564	65.898	34.981
1013	16.325	6.220	20.077	56.771	64.489	31.565
Sample Ch ₂ : $x = 0.53$; $u = 0.256137$, $S_{conf} = 15.431$ J/mol						
when $r_1 = [Fe^{3+}]$, $r_2 = [Al]$						
1225	9.068	4.824	23.727	16.485	12.552	30.347
1013	7.499	3.989	19.621	16.034	11.992	28.779
when $r_1 = 1 - ({}^{[4]}X_{Mg} + 2{}^{[6]}X_{Mg})$, $r_2 = 1/2({}^{[4]}X_{Al} + 2{}^{[6]}X_{Al})$						
1225	9.068	4.824	23.727	55.845	61.232	30.347
1013	7.499	3.989	19.621	55.394	60.671	28.779

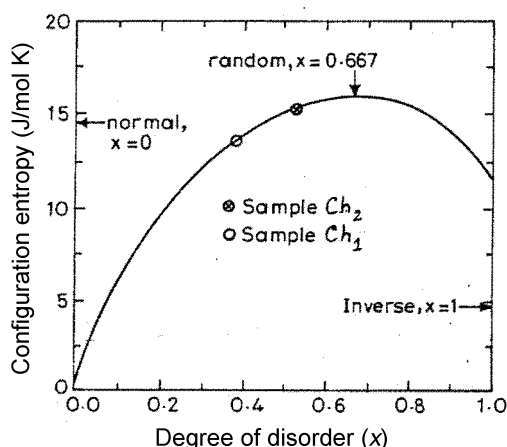


Figure 2. Sittampundi samples plotted in configurational entropy vs degree of disorder curve of Navrotsky and Klappa²⁹.

The compositional dependence of cation distribution in spinel is due to excess stabilization energy of divalent and trivalent cations in tetrahedral and octahedral sites³¹ and is expressed as ‘site preference enthalpy’^{8,9}. The compositional parameters (r_1 and r_2) of two independent compositional exchange vectors, $Fe^{2+}(Mg^{2+})^{-1}$ and $Al^{3+}(Fe^{3+} + Cr^{3+})^{-1}$ are $r_1 = 1 - ({}^{[4]}X_{Mg} + 2{}^{[6]}X_{Mg})$ and $r_2 = 1/2({}^{[4]}X_{Al} + 2{}^{[6]}X_{Al})$, where ${}^{[4]}X_{Al}$ and ${}^{[6]}X_{Al}$ are the atomic fraction of Al on tetrahedral and octahedral sites respectively. The site preference enthalpies a_1 and a_2 are calculated at the two temperatures from the following equations¹³:

$$-RT \ln \left[\frac{[Fe^{3+}]x(Fe^{2+})}{[Fe^{2+}]x(Fe^{3+})} \right] = a_1 + 2b_1[r_1 + r_2],$$

$$-RT \ln \left[\frac{[Al]x(Fe^{2+})}{[Fe^{2+}]x(Al)} \right] = a_2 + 2b_2[r_1 + r_2],$$

where $[Fe^{3+}] = Fe^{3+}$ at tetrahedral site and $(Fe^{3+}) = Fe^{3+}$ at octahedral site, and $b_1 = b_2 = -20$ kJ/mol. The two parameters (a_1 and a_2) are also calculated taking site occupancies (or order parameters r_1 and r_2) for $[Fe^{3+}]$ and $[Al]$ at the two metamorphic temperatures³²; the values are listed in Table 3.

These data bring out the significant aspect of measuring the relative site preference energy (with respect to Fe^{2+}) of aluminium at both tetrahedral and octahedral sites. Optical spectroscopic techniques widely used for determining the site preference crystal field stabilization energy delimit themselves with transition elements (3d and 4f) only, not covering amphoteric (non-transition elements like Al). The thermodynamic approach as employed herein may offer a cue for further studies with other amphoteric elements in mixed oxides.

Natural chromites are found to be a reciprocal system and Mg, Fe^{2+} , Al and Fe^{3+} are present in both the tetrahedral and octahedral sites. Cation distributions vary widely in the system. In the thermodynamic model proposed by O'Neill and Navrotsky⁸ for a spinel of intermediate cation distribution, the equation for free energy of disordering, $\Delta G_{dis} = x\Delta H_{int} - RT[x \ln x + (1-x)\ln(1-x) + x \ln(x/2) + (2-x)\ln(1-x/2)]$ has been obtained by combining the interchange enthalpy and configurational entropy. Using this equation, we have calculated the free energy of disordering of the two samples. For sample Ch₁, the values are 20.077 and 24.279 kJ/mol and for Ch₂, they are 23.727 and 19.621 kJ/mol respectively, at the two equilibrium temperatures.

Change in configurational entropy in disordering (ΔS_{conf}) is also determined at the two temperatures using the equa-

tion: $\Delta G_{\text{dis}} = x(\mathbf{a} + \mathbf{b}x) - T(\Delta S_{\text{conf}} + \Delta S_{\text{nonconf}})$ (see Table 3). The configurational entropy term ($\Delta S_{\text{nonconf}}$) is too small and is neglected. In the ordered state, ΔS_{conf} is equal to the configurational entropy (S_{conf}).

1. Andreozzi, G. B. and Princivalle, F., Kinetics of cation ordering in synthetic MgAl_2O_4 spinel. *Am. Mineral.*, 2002, **87**, 838–844.
2. Foley, J. A., Wright, S. E. and Hughes, J. M., Cation partitioning versus temperature in spinel: Optimization of site occupants. *Phys. Chem. Miner.*, 2001, **28**, 143–149.
3. Hålenius, U., Skogby, H. and Andreozzi, G. B., Influence of cation distribution on the optical absorption spectra of Fe^{3+} -bearing spinel s.s.-hercynite crystals: evidence for electron transitions in ${}^{\text{VI}}\text{Fe}^{2+}$ - ${}^{\text{VI}}\text{Fe}^{3+}$ clusters. *Phys. Chem. Miner.*, 2002, **29**, 319–330.
4. Nell, J., Wood, B. J. and Mason, T. O., High temperature cation distributions in Fe_3O_4 - MgAl_2O_4 - MgFe_2O_4 - $\text{Fe}_2\text{Al}_2\text{O}_4$ spinels from thermopower measurements. *Am. Mineral.*, 1989, **74**, 339–351.
5. Carpenter, M. A. and Salje, E. K. H., Thermodynamics of nonconvergent cation ordering in minerals: II. Spinels and orthopyroxene solid solution. *Am. Mineral.*, 1994, **79**, 1068–1083.
6. Lehmann, J. and Roux, J., Experimental and theoretical study of $(\text{Fe}^{2+}, \text{Mg})(\text{Al}, \text{Fe}^{3+})_2\text{O}_4$ spinels: Activity–composition relationships, miscibility gaps, vacancy contents. *Geochim. Cosmochim. Acta*, 1986, **50**, 1765–1783.
7. Nell, J. and Wood, B. J., High temperature electrical measurements and thermodynamic properties of Fe_3O_4 – FeCr_2O_4 – MgCr_2O_4 – FeAl_2O_4 spinels. *Am. Mineral.*, 1991, **76**, 445–457.
8. O'Neill, H. St. C. and Navrotsky, A., Simple spinels: Crystallographic parameters, cation radii, lattice energies and cation distribution. *Am. Mineral.*, 1983, **68**, 181–194.
9. O'Neill, H. St. C. and Navrotsky, A., Cation distributions and thermodynamic properties of binary spinel solid solutions. *Am. Mineral.*, 1984, **69**, 733–753.
10. Redfern, S. A. T., Harrison, R. J., O'Neill, H. St. C. and Wood, R. R., Thermodynamics and kinetics of cation ordering in MgAl_2O_4 spinel up to 1600°C from *in situ* neutron diffraction. *Am. Mineral.*, 1999, **84**, 299–310.
11. Subramaniam, A. P., Mineralogy and petrology of the Sittampundi complex, Salem district, Madras State, India. *Bull. Geol. Soc. Am.*, 1956, **67**, 317–390.
12. Bidyananda, M. and Mitra, S., Room temperature ${}^{57}\text{Fe}$ Mössbauer characteristics of chromites from the Nuggihalli schist belt, Dharwar craton, southern India. *Curr. Sci.*, 2004, **86**, 101–106.
13. Wood, B. J. and Virgo, D., Upper mantle oxidation state: Ferric iron contents of lherzolite spinels by ${}^{57}\text{Fe}$ Mössbauer spectroscopy and resultant oxygen fugacities. *Geochim. Cosmochim. Acta*, 1989, **57**, 1277–1291.
14. Dyar, M. D., McGuire, A. V. and Zeigler, R. D., Redox equilibria and crystal chemistry of coexisting minerals from spinel lherzolite mantle xenoliths. *Am. Mineral.*, 1989, **74**, 969–980.
15. Fatseas, G. A., Dormann, J. L. and Blanchard, H., Study of the $\text{Fe}^{3+}/\text{Fe}^{2+}$ ratio in natural chromites $(\text{Fe}_x\text{Mg}_{1-x})(\text{Cr}_{1-y-x}\text{Fe}_y\text{Al}_x)\text{O}_4$. *J. Phys.*, 1976, **12**, 787–792.
16. Galvao Da Silva, E., Aloras, A. and Speziali, N. Z., Mössbauer effect study of natural chromites of Brazilian and Philippine origin. *Appl. Phys.*, 1980, **22**, 389–392.
17. Marshall, L. and Dollase, W., Cation arrangement in Fe–Zn–Cr spinel oxides. *Am. Mineral.*, 1984, **69**, 928–936.
18. Mitra, S., Pal, T. and Pal, T. N., Electron localisation at B-site a concomitant process for oxidation of Cr-spinels to a partly inverse form. *Solid State Commun.*, 1991, **77**, 297–301.
19. Mitra, S., Pal, T. and Pal, T. N., Petrogenetic implication of the Mössbauer hyperfine parameters of Fe^{3+} -chromites from Sukinda (India) ultramafites. *Mineral. Mag.*, 1991, **55**, 535–542.
20. Pal, T., Moon, H. S. and Mitra, S., Distribution of cations in natural chromites at different stages of oxidation – A ${}^{57}\text{Fe}$ Mössbauer investigation. *J. Geol. Soc. India*, 1994, **44**, 53–64.
21. Osborne, M. D., Fleet, M. E. and Bancroft, G. M., Fe^{2+} – Fe^{3+} ordering chromite and Cr-bearing spinels. *Contrib. Mineral. Petrol.*, 1981, **77**, 251–255.
22. Osborne, M. D., Fleet, M. E. and Bancroft, G. M., Next-nearest-neighbour effects in the Mössbauer spectra of (Cr, Al) spinel. *J. Solid State Chem.*, 1984, **53**, 174–183.
23. Galvao Da Silva, E., Aloras, A. and Sette Camara, A. O. R., Mössbauer effect study of cation distribution in natural chromites. *J. Phys.*, 1976, **12**, 783–785.
24. Singh, A. K., Jain, B. K., Date, S. K. and Chand, A. K., Structural and compositional study of natural chromites of Indian origin. *Appl. Phys.*, 1978, **11**, 769–776.
25. Ellis, D. J. and Green, D. H., An experimental study of the effect of Ca upon garnet clinopyroxenes Fe–Mg exchange equilibria. *Contrib. Mineral. Petrol.*, 1979, **71**, 13–22.
26. Harrison, R. J., Redfern, S. A. T. and O'Neill, H. St. C., The temperature dependence of the cation distribution in synthetic hercynite (FeAl_2O_4) from *in situ* neutron structure refinements. *Am. Mineral.*, 1998, **83**, 1092–1099.
27. Mozzi, R. L. and Paladino, A. E., Cation distributions in non-stoichiometric magnesium ferrite. *J. Chem. Phys.*, 1963, **39**, 148–162.
28. Lenaz, D., Andreozzi, G. B., Mitra, S., Bidyananda, M. and Princivalle, F., Crystal chemical and ${}^{57}\text{Fe}$ Mössbauer study of chromite from the Nuggihalli schist belt (India). *Mineral. Petrol.*, 2004, **80**, 45–57.
29. Navrotsky, A. and Kleppa, O. J., The thermodynamics of cation distributions in simple spinels. *J. Inorg. Nucl. Chem.*, 1967, **29**, 2701–2714.
30. Navrotsky, A., Repeating patterns in mineral energetics. *Am. Mineral.*, 1994, **79**, 589–605.
31. Della Giusta, A. and Ottonello, G., Energy and long-range disorder in simple spinels. *Phys. Chem. Miner.*, 1993, **20**, 228–241.
32. O'Neill, H. St. C. and Wall, V. J., The olivine-orthopyroxene-spinel oxygen geobarometer the nickel precipitation curve, and the oxygen fugacity of the earth's upper mantle. *J. Petrol.*, 1987, **28**, 1169–1191.

ACKNOWLEDGEMENTS. We thank Prof. H. S. Moon, Yonsei University, Seoul for cooperation in EPMA analysis of the samples. Dr S. Annadurai is acknowledged for his cooperation in the field as well as in laboratory studies. The University Grants Commission, New Delhi is acknowledged for financial support to S. M. and A. K. S.; M. B. thanks the Department of Science and Technology, New Delhi for a research grant under the Fast Track Young Scientist Scheme.

Received 29 April 2005; revised accepted 18 October 2005